Bull. Mater. Sci., Vol. 36, No. 7, December 2013, pp. 1147–1151. © Indian Academy of Sciences.

Yb^{3+} and Er^{3+} co-doped $Y_2Ce_2O_7$ nanoparticles: synthesis and spectroscopic properties

HONGHUI JIANG, WEIXIONG YOU*, XIAOLIN LIU, JINSHENG LIAO, PING WANG and BIN YANG

School of Material Science and Engineering, Jiangxi University of Science and Technology, Ganzhou 341000, P. R. China

MS received 22 July 2011; revised 21 November 2012

Abstract. **Yb^{3+} and Er^{3+} co-doped $Y_2Ce_2O_7$ nanoparticles sintered at different temperatures were prepared by homogeneous co-precipitation method. The products were characterized by X-ray powder diffraction (XRD), energy-dispersive spectroscopy (EDS) and transmission electron microscopy (TEM). The results indicated that the particle sizes and morphologies of the samples were heavily influenced by the sintering temperature. As temperature increased, the particle sizes became gradually larger and more agglomerate. The emissions including green and red upconversion emissions were investigated under 980 nm excitation. The emission intensities of the samples also depended on the sintering temperature. Two photon processes were mainly responsible for green and red upconversion emissions.**

Keywords. **Nanoparticles; Yb^{3+} and Er^{3+}; $Y_2Ce_2O_7$; upconversion emissions.**

1. Introduction

Upconversion is an anti-Stokes process where low energy photon is converted to higher energy photon. During the past decades, upconversion fluorescence materials have attracted much attention due to their potential applications in display technology, bioimaging and upconversion lasers (de Sousa *et al* 1999; Liu and Chen 2007; Qian *et al* 2009). Trivalent rare earth (RE) ions such as Er^{3+}, Tm^{3+} and Ho^{3+} are doped as emission centres in these materials. Among these rare earth ions, Er^{3+} ion is the most popular and efficient ion for upconversion because it can be conveniently populated by commercial low-cost high-power 980 nm laser diode (Guo 2007; Xu *et al* 2010). In addition, Er^{3+} ion has abundant energy level structure, so green and red upconversion emissions can be realized in Er^{3+}-doped materials. In order to improve the pumping efficiency of upconversion, another ion is usually introduced into the host materials as a sensitizer. Yb^{3+} ion is an excellent candidate for sensitizer because it has a broad and high absorption band around the 980 nm pump wavelength. In the Yb^{3+} and Er^{3+} co-doped systems, the pumping energy can be absorbed by Yb^{3+} efficiently and transferred to the Er^{3+} ion to enhance the emission intensities. Furthermore, the Yb^{3+} ion has only two energy levels, which excludes its other excited state absorption or upconversion losses in principle (Cantelar *et al* 1998; da Vila *et al* 2003).

The $A_2B_2X_7$ pyrochlore structure is a cation and anion vacancy ordered derivative of fluorite structure. In the $A_2B_2X_7$ pyrochlore structure, the A and B cations are located on 16c (0, 0, 0) and 16d (1/2, 1/2, 1/2) positions, respectively,the X anions occupy the 48f (3/8, 1/8, 1/8) and 8a (1/8, 1/8, 1/8) positions (Reid *et al* 2012). Pyrochlore compounds have many properties and can be put forward as materials for use in diverse applications including catalysts (Korf *et al* 1987; Tong *et al* 2008), thermal barrier coatings (Vassen *et al* 2000), solid electrolytes (Heremans *et al* 1995) and nuclear waste forms (Sickafus *et al* 2000). However, there are few reports on the photoluminescence properties of the rare earth-doped $A_2B_2X_7$ compounds. In this paper, we concentrate our attention on the preparation and spectroscopic properties of Yb^{3+} and Er^{3+} co-doped $Y_2Ce_2O_7$ phosphors. In order to obtain the aimed-precursor, homogeneous co-precipitation reaction is adopted. The effects of sintering temperature on the spectroscopic properties of Yb^{3+} and Er^{3+} co-doped $Y_2Ce_2O_7$ nanoparticles have been studied.

2. Experimental

All the chemicals of Y_2O_3 (99·99%), CeO_2 (99·99%), Yb_2O_3 (99·99%), Er_2O_3(99·99%), $(NH_2)_2CO$ (AR), HNO_3 and H_2O_2 were used as starting raw materials without any further

*Author for correspondence (you_wx@126.com)

purification. $(NH_2)_2CO$ was dissolved in deionized water under magnetic stirring at 40 °C, and the solution was continuously stirred until a clear solution was obtained. Then, according to the formula, $Y_{1.94}Yb_{0.04}Er_{0.02}Ce_2O_7$, stoichiometric amounts of starting materials Yb_2O_3, Er_2O_3, Y_2O_3 and CeO_2 were successively added into dilute nitric acid under heating. All of these rare-earth oxides were completely dissolved by slowly dropping H_2O_2 and finally obtained rare-earth nitrates solution. The co-precipitation reaction started when the as-prepared $(NH_2)_2CO$ solution was slowly added to the above rare-earth nitrates solution. The resultant solution was stirred for about 2 h at 90 °C, and then white precursor was formed. After cooling to room temperature, the white precursor was collected by centrifugation and washed with deionized water. The precursor was sintered at certain temperature (1000, 1100, 1200, and 1300 °C) for 4 h in air to yield the Yb^{3+} and Er^{3+} co-doped $Y_2Ce_2O_7$ products.

X-ray powder diffraction (XRD) patterns of the as-prepared samples were recorded using a Rigaku D/MAX-RB X-ray diffractometer with high-intensity CuKα radiation (λ = 1·54178 Å). Transmission electron microscopy (TEM) micrographs were taken with a Tecnai F20 field-emission transmission electron microscope. The emission spectra were detected using spectrophotometer (FLS920, Edinburgh) with Xenon lamp and laser diode (LD) as the pump sources and the excitation wavelength was 980 nm. The signal was detected with a NIR PMT (R5509, Hamamatsu). All measurements were carried out at room temperature and all the spectra had been corrected.

3. Results and discussion

Figure 1 shows XRD patterns of the samples prepared by precursor thermal transformation for 4 h at 1000, 1100, 1200, and 1300 °C, respectively. The peaks are in good agreement with the standard data (JCPDS no. 09-0286), which means that the crystal structure belongs to the cubic system with space group *Fm3m*. No diffraction peaks from impurities were observed in XRD patterns, indicating that pure single-phase $Y_2Ce_2O_7$ can be obtained at temperature from 1000 to 1300 °C and the temperature over 1000 °C has no effect on the crystal phase of the products. Furthermore, the peaks do not shift in different samples, which indicate that the Yb^{3+} and Er^{3+} have invaded into the crystal lattices without any crystal structure distortion. The element analysis of energy-dispersive spectroscopy (EDS) (shown in figure 2) of the sample also proves that Yb^{3+} and Er^{3+} ions are successfully doped into $Y_2Ce_2O_7$ at 1000 °C. Because the XRD patterns do not show diffraction peaks of Er_2O_3 and Yb_2O_3 crystalline phase, Yb^{3+} and Er^{3+} were completely co-doped into the crystal structure and substituted for Y^{3+} ions.

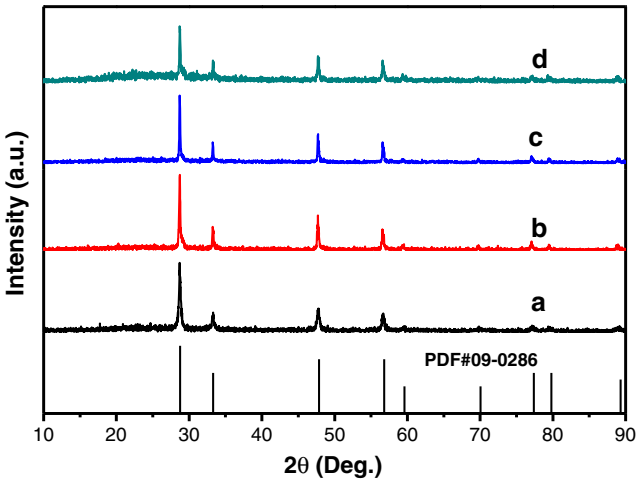

Figure 1. XRD patterns of Yb^{3+} and Er^{3+} co-doped $Y_2Ce_2O_7$ nanoparticles prepared for 4 h at different sintering temperatures: (**a**) 1000 °C, (**b**) 1100 °C, (**c**) 1200 °C and (**d**) 1300 °C.

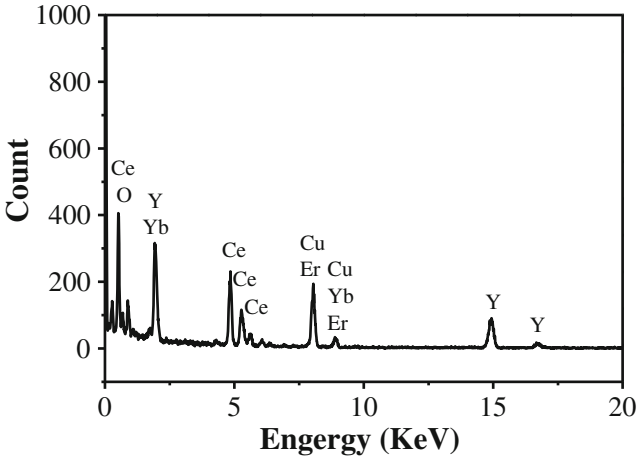

Figure 2. Energy dispersive spectra of Yb^{3+} and Er^{3+} co-doped $Y_2Ce_2O_7$ nanoparticles prepared for 4 h at 1000 °C.

Figure 3(a–d) shows typical TEM micrographs of the as-prepared sample. It can be seen that the sizes of Yb^{3+} and Er^{3+} co-doped $Y_2Ce_2O_7$ nanoparticles range from tens of nanometers to several hundred nanometers. Moreover, the particle sizes and morphologies are heavily influenced by the sintering temperatures. As temperature increased, the particle sizes became gradually larger and more agglomerated. The reason may be due to the fact that the crystal will grow faster in higher temperature.

Figure 4 shows emission spectra of the samples in the range of 1400–1700 nm with the excitation wavelength at 980 nm by Xenon lamp. These emission bands are

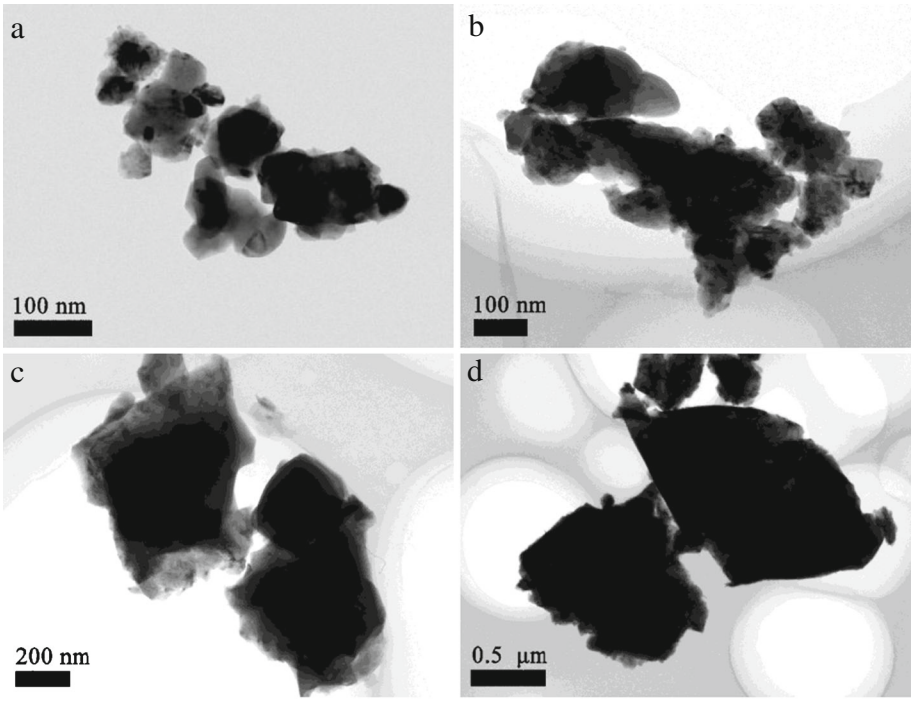

Figure 3. TEM micrographs of Yb^{3+} and Er^{3+} co-doped $Y_2Ce_2O_7$ nanoparticles prepared at different sintering temperatures: (**a**) 1000 °C, (**b**) 1100 °C, (**c**) 1200 °C and (**d**) 1300 °C.

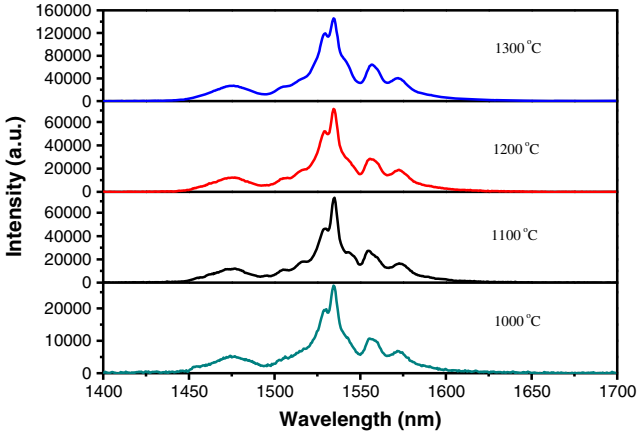

Figure 4. Emission spectra of Yb^{3+} and Er^{3+} co-doped $Y_2Ce_2O_7$ nanoparticles prepared by thermal treatment at 1000, 1100, 1200 and 1300 °C (under 980 nm excitation).

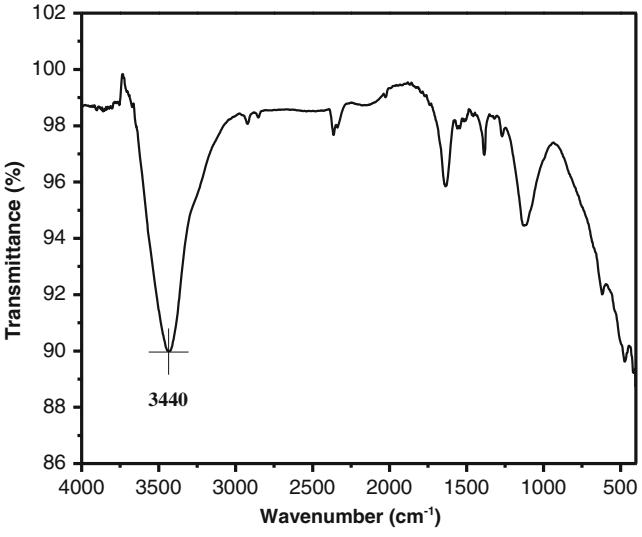

Figure 5. Infrared spectrum of Yb^{3+} and Er^{3+} co-doped $Y_2Ce_2O_7$ nanoparticles prepared at 1000 °C.

attributed to the $^4I_{13/2} \rightarrow {}^4I_{15/2}$ transition of Er^{3+} ion and the emission peaks are located at 1535 nm. It can be seen from the figure that the emission intensities are heavily affected by the sintering temperature. From 1000 to 1300 °C, the emission intensities increase with increasing sintering temperature. The reason may be due to three factors: (a) as mentioned above, the particle sizes become larger when the temperature increases, which produces less scattering and dissipation of light, causing enhancement of photoluminescence intensities (Jeong *et al* 2003; Chen *et al* 2011), (b) the defects in the crystals may decrease with increasing temperature, so the energy losses caused

by the defects can be reduced and the emission intensities enhanced, and (c) the reduction of hydroxyl groups in the samples. Figure 5 shows infrared spectrum of the Yb^{3+} and Er^{3+} co-doped $Y_2Ce_2O_7$ nanoparticles prepared at 1000 °C. The peaks located at 3440 cm^{-1} belongs to the absorption of OH group. The amount of OH group decreases with the increase of sintering temperature, which lowers the multi-phonon relaxation rate (Ghosh and Patra 2006) and then the emission intensities enhanced. In addition, the loss of hydroxyl groups may be the dominant factor to increase the emission intensity with the increase of sintering temperature.

Figure 6 shows upconversion photoluminescence spectra of the Yb^{3+} and Er^{3+} co-doped $Y_2Ce_2O_7$ nanoparticles under 980 nm excitation by LD. The green emissions

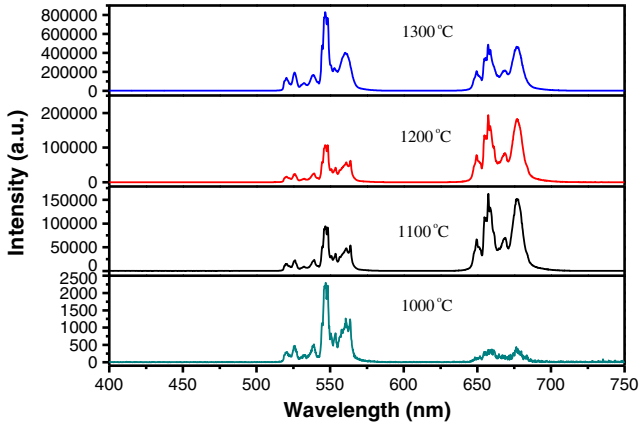

Figure 6. Upconversion spectra of Yb^{3+} and Er^{3+} co-doped $Y_2Ce_2O_7$ nanoparticles prepared by thermal treatment at 1000, 1100, 1200 and 1300 °C (under 980 nm excitation).

located at 525 and 546 nm correspond to $^2H_{11/2} \rightarrow {}^4I_{15/2}$ and $^4S_{3/2} \rightarrow {}^4I_{15/2}$ transitions. Similarly, the red emission located at 656 nm is assigned to $^4F_{9/2} \rightarrow {}^4I_{15/2}$ transition. In the Yb^{3+} and Er^{3+} co-doped materials, mechanism for green upconversion emissions should be the resonant energy transfer (ET) upconversion (You *et al* 2012). As shown in figure 7, the Yb^{3+} ion can be excited to the $^2F_{5/2}$ level by absorbing one 980 nm photon and then transferred the energy to Er^{3+} ion, exciting Er^{3+} ion to the excited $^4I_{11/2}$ level. The Er^{3+} ion on $^4I_{11/2}$ level will be promoted to $^4F_{7/2}$ level by energy transfer (ET) from the relaxation of another excited Yb^{3+} ion. The Er^{3+} ions on $^4F_{7/2}$ level will decay nonradiatively to $^2H_{11/2}$ and $^4S_{3/2}$ levels, the green emissions can be derived when the Er^{3+} ions on these two levels relax to the ground $^4I_{15/2}$ level (You *et al* 2012). For the red upconversion emissions, the Er^{3+} ion on $^4F_{7/2}$ level will decay nonradiatively to $^4F_{9/2}$ level, or part of $^4I_{11/2}$ level will relax nonradiatively to $^4I_{13/2}$ level and then three transition processes happened (Xu *et al* 2010):

$$\text{ESA}: {}^4I_{13/2}(\text{Er}) + \text{a photon} \rightarrow {}^4F_{9/2}(\text{Er}),$$

$$\text{CR}: {}^4I_{13/2}(\text{Er}) + {}^4I_{11/2}(\text{Er}) \rightarrow {}^4F_{9/2}(\text{Er}) + {}^4I_{15/2}(\text{Er}),$$

$$\text{ET}: {}^4I_{13/2}(\text{Er}) + {}^2F_{5/2}(\text{Yb}) \rightarrow {}^4F_{9/2}(\text{Er}) + {}^2F_{7/2}(\text{Yb}).$$

The radiative transition from $^4F_{9/2}$ to $^4I_{15/2}$ level emits red emission. Obviously, two or more ions (Yb^{3+} and Er^{3+}) are involved in these transition processes. It is well known that these transition processes depend on the distance between two ions. If the distance between two ions is too large, the transition processes cannot happen. In figure 6, the green and red emission intensities increase with the increase of thermal

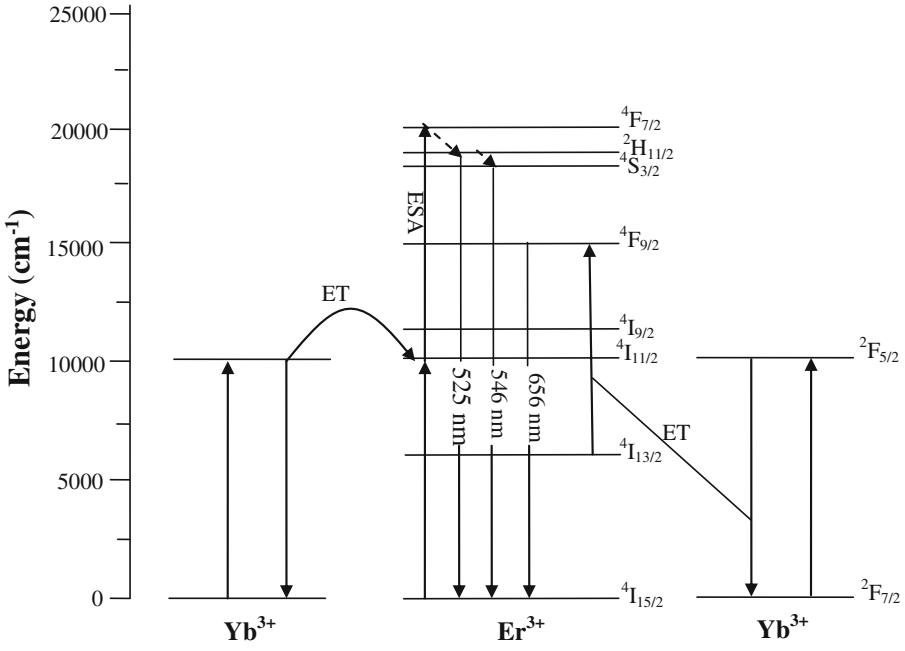

Figure 7. Energy level diagrams of Yb^{3+} and Er^{3+} for upconversion emissions under 980 nm excitation.

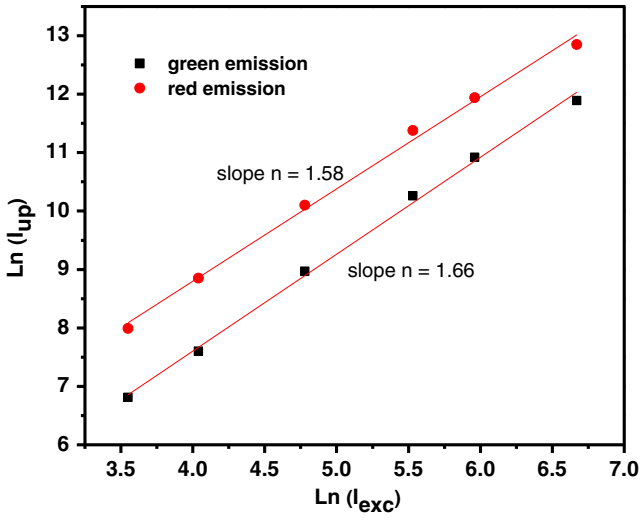

Figure 8. ln–ln plots of green and red emissions of Yb^{3+} and Er^{3+} co-doped $Y_2Ce_2O_7$ nanoparticles prepared at 1300 °C excitation laser power (980 nm excitation wavelength).

treating temperatures. The reason may be due to two factors mentioned above. However, for the samples sintered at 1000 and 1300 °C, the green emission intensities are higher than the red ones, which are contrary to the results obtained in the samples sintered at 1100 and 1200 °C. The reason may be due to the random distribution of Yb^{3+} and Er^{3+} ions caused by the temperature in different samples, so distances between Yb^{3+} and Er^{3+} are irregular and upconversion intensities become disordered. This suggestion will be thoroughly investigated in our further work.

It is known that the number of photons required for upconversion processes can be evaluated by the following relation (Pollnau *et al* 2000):

$$I_{\text{up}} \propto (I_{\text{exc}})^n,$$

where I_{up} and I_{exc} represent the upconversion emission intensity and the pump laser power, respectively and n is the number of photons required to produce an upconversion photon. Figure 8 shows excitation power dependence of the green and red emissions of Yb^{3+} and Er^{3+} co-doped $Y_2Ce_2O_7$ nanoparticles prepared at 1300 °C. The values of slopes for the green and red upconversion emissions are 1·66 and 1·58, respectively. The result indicates that two photon processes are mainly responsible for green and red upconversion emissions.

4. Conclusions

In summary, Yb^{3+} and Er^{3+} co-doped $Y_2Ce_2O_7$ nanoparticles have been successfully synthesized at 1000, 1100, 1200 and 1300 °C. The grain sizes of Yb^{3+} and Er^{3+} co-doped $Y_2Ce_2O_7$ nanoparticles can be manipulated by sintering temperature. The bright green and red upconversion emissions (nm) can be observed under 980 nm excitation. With the increase of sintering temperatures, the particle sizes and emission intensities increase. The relative intensities of green and red emission are varied with sintering temperature. The mechanism for green and red upconversion emissions are two photons processes. Therefore, these Yb^{3+} and Er^{3+} co-doped $Y_2Ce_2O_7$ nanoparticles may be promising upconversion materials.

Acknowledgments

This work has been supported by the National High Technology Research and Development Program of China (2010AA03A408), the National Natural Science Foundation of China (51062004), the Natural Science Foundation of Jiangxi Province (2009GQC0038) and Scientific Research Foundation for universities from Education Bureau of Jiangxi Province (GJJ10165).

References

Cantelar E, Munoz J A, Sanz-Garcia J A and Cusso F 1998 *J. Phys: Condens. Matter* **29** 1840
Chen H, Yang B, Sun Y, Zhang M F, Sui Y, Zhang Z and Cao W 2011 *J. Lumin.* **131** 2574
da Vila L D, Gomes L, Tarelho L V G, Ribeiro S J L and Messadeq Y 2003 *J. Appl. Phys.* **93** 3873
de Sousa D F, Zonetti L F C, Bell M J V, Lebullenger R, Hemandes A C and Nunes L A O 1999 *J. Appl. Phys.* **85** 2502
Ghosh P and Patra A 2006 *Langmuir* **22** 6321
Guo H 2007 *Opt. Mater.* **29** 1840
Heremans C, Wuensch B J, Stalick J K and Prince E 1995 *J. Solid State Chem.* **117** 108
Jeong J H, Bae J S, Yi S S, Park J C and Kim Y S 2003 *J. Phys. Condens. Matter* **15** 567
Korf S J, Koopmans H J A, Lippens B C, Burggraaf A J and Gellings P J 1987 *J. Chem. Soc., Faraday Trans.* **83** 1485
Liu C and Chen D 2007 *J. Mater. Chem.* **17** 3875
Pollnau M, Gamelin D R, Luthi H U and Hehlen M P 2000 *Phys. Rev.* **B61** 3337
Qian H, Guo H, Ho P C, Mahendran R and Zhang Y 2009 *Small* **5** 2285
Reid D P, Stennett M C and Hyatt N C 2012 *J. Solid State Chem.* **191** 2
Sickafus K E, Minervini L, Grimes R W, Valdez J A, Ishimaru M, Li F, McClellan K J and Hartmann T 2000 *Science* **289** 748
Tong Y, Xue P, Jian F, Lu L, Wang X and Yang X 2008 *Mater. Sci. Eng.* **B150** 194
Vassen R, Cao X, Tietz F, Basu D and Stover D 2000 *J. Am. Ceram. Soc.* **83** 2023
Xu C, Yang Q, Ren G and Liu Y 2010 *J. Alloy Compd.* **503** 82
You W, Lai F, Jiang H and Liao J 2012 *Phys* **B407** 1094